IJE TRANSACTIONS C: AspectsVol. 27, No. 9, (September 2014) 1359-1366

International Journal of Engineering

Journal Homepage: www.ije.ir

Magnetic Saturation Impacts on Fault Analysis of Squirrel-cage Six Phases Induction Motors Using Winding Function Approach

A. Taheri, M. Sabouri*

Department of Electrical Engineering, University of Zanjan, Zanjan, Iran

PAPER INFO

Paper history:
Received 10 November 2013
Received in revised form 15 March 2014
Accepted 22 May 2014

Keywords:
6-Phases Squirrel-cage Induction Motors
Saturation Effect
Rotor Fault
Stator Fault
Winding Function Approach

ABSTRACT

Multiple coupled circuit modeling (MCCM) of squirrel-cage induction motors (SCIMs), or winding function approach is the most detailed and complete analytical model used to analyze the performance of faulty SCIMs. Already, in various papers this approach has been used for 3-phases SCIMs, but this paper extends the above-mentioned model to 6-phases SCIMs. Various simulations of variative faults were carried out on faulty 6-phases SCIMs, and then, results obtained fromthe simulation were presented. The innovation of this paper is the first time simulation of broken bars and stator winding faults on 6-phases SCIMs using winding function approach with considering magnetic saturation effect that precise results were obtained as presented.

doi: 10.5829/idosi.ije.2014.27.09c.05

1. INTRODUCTION

For economic utilization of the magnetic material, operating regions of electrical machines have to be extended above the knee of the magnetization characteristic, which forces the machine into saturation. Therefore, many attempts have been made to include saturation effects in squirrel-cage induction machine (SCIM) models [1-5]. The multiple coupled circuits model (MCCM) of SCIM, based on the winding function theory [6-10] is one of these models. MCCM has gained a wide application in the analysis of SCIM, mainly due to its ability to analyze faulty machines. Such analysis helps to realize the faulty SCIMs performance, to extract proper indexes for various faults and to develop effective fault diagnosis and condition monitoring techniques for the SCIMs. As the magnetic saturation may have considerable effect on the performance of SCIMs and their fault indexes [11, 12], it is reasonable to include saturation effect to MCCM properly. An extension to MCCM, which includes variable degrees of saturation effects, has been reported in the literature[5]. The proposed saturable MCCM (SMCCM) needs to track the air gap rotating flux density, and this has been done by a rather simple technique n [5]. However, application of that technique may lead to a wrong result if the air gap flux distribution is distorted. As it will be clear in the next sections, many SCIM faults cause the air gap flux density to be disturbed. Thus, existing SMCCM is not viable to analyze faulty SCIMs. In addition, the saturation factor (K_{sat}) has been determined using air gap voltage fundamental harmonic amplitude [5], which depends on the rotation speed of the air gap flux density as well as its amplitude, while the saturation degree depends only on the flux density amplitude.In this paper, according to technique proposed in the literature[13], flux-linkages of rotor meshes, which are calculated in every simulation step, are used to estimate the air gap flux density distribution around the air gap. Then, Fourier series analysis is used to determine the space harmonics of the air gap flux density. Beside, multiphase machines of various types have received great deal of attention. Space-harmonic in a multiphase

*Corresponding Author's Email: Taheri@znu.ac.ir (A. Taheri)

Please cite this article as:A. Taheri and M. Sabouri, N. Sathurappan, Magnetic Saturation Impacts on Fault Analysis of Squirrel-cage Six Phases Induction Motors using Winding Function Approach,, International Journal of Engineering (IJE), TRANSACTIONS C: Aspects Vol. 27, No. 9, (September 2014) 1359-1366

machine is less than 3-phase machine. Also, the redundancy in a multiphase machine is greater than 3-phase one [14-16]. One of the most interesting multiphase machines is the 6–phase induction.

2. SATURABLE MULTIPLE COUPLED CIRCUIT MODEL OF SQUIRREL-CAGE INDUCTION MACHINES

According to the winding function or modified winding function theories defined in the literature[13], inductances between stator phases, rotor bars and mutual inductances between stator phases a and rotor meshes are calculated as follows:

$$L_{xy} = m_o r l \int_0^{2p} g^{-1} n_x N_y \, dj \quad (1)$$

where x and y can be any phase of the stator or any mesh of the rotor, μ_o is the air magnetic permeability, r is the air gap mean radius, l is the stack length, g^{-1} is the inverse air gap function, n_x is the x phase (mesh) turn function and φ is the angle in the stator stationary reference frame. In the case of uniform air gap, N_y is the winding function of y phase (mesh). Figure 1 shows the air gap flux density distribution and its fundamental space harmonic for a SCIM with two broken rotor bars. Distortion of the flux density due to the fault is obvious in the figure.

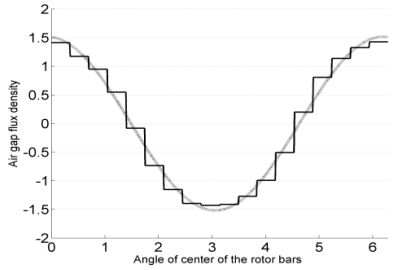

Figure 1. Fundamental space harmonic (---) for a SCIM with two broken rotor bars.Estimated air gap flux density (__)

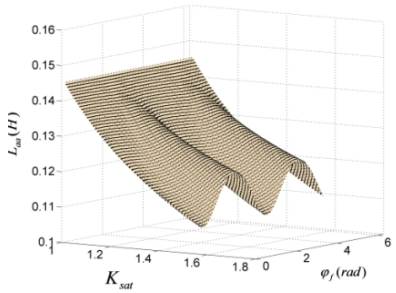

Figure 2. Stator phase "a" self inductance (L_{aa}) variation versus K_{sat} and j_f

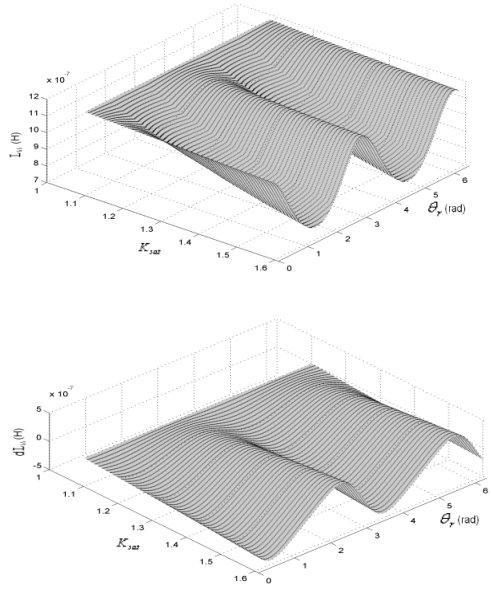

Figure 3. Rotor mesh "1" self inductance (L_{11} —top) and its derivative versus (dL_{11} —bottom) variations versus K_{sat} and θ_r where $j_f = 0$.

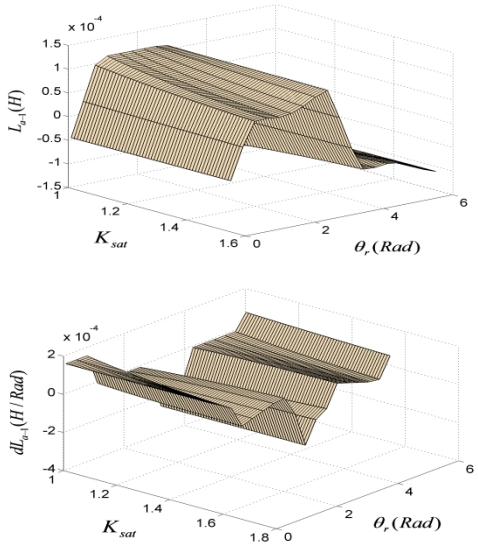

Figure 4. The mutual inductance between stator phase "a" and rotor mesh "1"(L_{a1} —top) and its derivative versus (dL_{a1}—bottom) variations versus K_{sat}

An 1HP, 380V, 50Hz, 2-poles, 6-phases, Y-connected general purpose SCIM was simulated using SMCCM. Figures 2 and 3 represent, respectively, the variation of self inductance of the stator phase "a" (L_{aa}) and self inductance of the rotor mesh 1 (L_{11}) plus its derivative versus θ_r (dL_{11}) and Figure 4 shows the mutual inductance between stator phase "a" and rotor mesh 1 (L_{a1}) plus its derivative versus θ_r (dL_{a1}) for a 2-pole CIM. As seen, by increasing saturation factor (K_{sat})

, L_{aa} and L_{11} fluctuate increasingly around decreasing the mean value while dL_{11} fluctuates around zero.

3. 6-PHASES SCIM PERFORMANCE DUE TO MAGNETIC SATURATION UNDER BROKEN ROTOR BARS

Many kinds of stresses on a SCIM may lead to rotor bars breakage, including thermal stresses, magnetic stresses, residual stresses, dynamic stresses, environmental stresses and mechanical stresses [17]. 5% -10% of total SCIMs failures are due to the rotor faults and considerable research reports, aiming at diagnosis of these faults are available in the literature [17]. Here the SCIM performance under broken rotor bars is studied using SMCCM and compared to those obtained by MCCM. So, the magnetic saturation effect on the performance will be clear. As mentioned previously, many faults, such as rotor broken bars, may disturb the air gap flux density distribution (see Figure1), and this intensifies the space harmonics of the air gap flux density.

Magnetization curve of the motor was determined by experiments as well as simulation and shown in Figure 5. As seen, the nominal voltage of the motor is above knee-point of the magnetization curve. In both figures, simulation and experimental results agree well and this implies the high accuracy of the developed SMCCM. The SMCCM results in Figure 5 are qualitatively in agreement with the corresponding experimental results[18]. Figure 6 shows the rotor teeth flux densities determined by a manner described in section III assuming the total flux passing through any rotor mesh isconcentrated in relevant rotor tooth uniformly. As seen, a broken rotor bar has reduced the flux of an adjacent tooth and increased the flux of other adjacent tooth considerably.

This leads to a higher local saturation in the later tooth. Saturation effect on the teeth flux densities is obvious in the figure and is in agreement with the similar finite elements results [18].The influence of a rotor broken bar on the stator line current of SCIM can be realized using an approach based on rotating magnetic fields. For positive-sequence supply voltage, the stator windings produce a magnetic field in the air gap, which rotates at synchronous speed (ω_s) in forward direction.

The rotor rotating at $\omega_m=(1-s)\omega_s$, is therefore seeing the rotating field at speed sωs, where s is the slip. Thus, currents at frequency sf are induced and flow in the rotor bars, where f is the supply frequency.A broken bar, whose current reduces to zero, can be represented as the superposition of a healthy bar and a current source injecting, at all times, a current in the bar of opposite value as the current flowing in the healthy bar [18, 19].

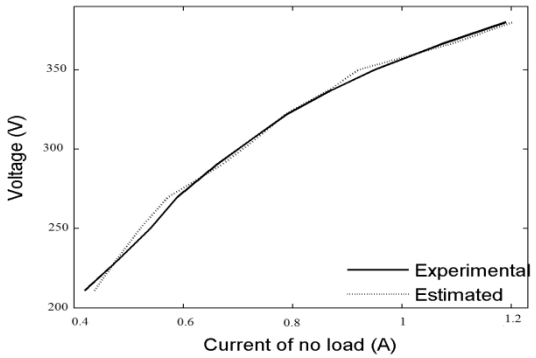

Figure 5. Stator line voltage versus no-load current (magnetization curve) obtained by simulation using SMCCM (__) and experiment (×).

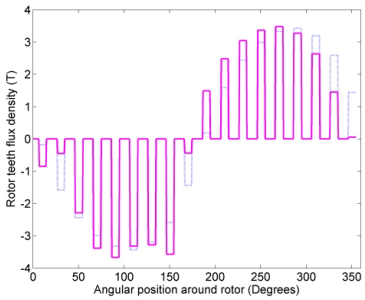

Figure 6. Estimated rotor teeth flux densities in healthy (---) and 6 broken bar (__) CIMs obtained by simulation.

This superimposed current (current source) creates a superimposed pulsating field of pulsation $s\omega_s$ with regard to the rotor. This pulsating field can be split in two rotating fields of opposite directions; the forward field, rotating at $s\omega_s$with respect to the rotor, and therefore, at ω_s with regard to the stator windings, which affects the value of the fundamental stator currents, and the backward field, rotating at $(1-2s)\omega_s$with respect to the stator windings, induces currents at frequency $(1-2s)f$ in the stator windings. Furthermore, in this situation, the torque has a component fluctuating at frequency $2sf$, which creates speed ripple at the same frequency. This finally results in inducing the currents at frequency $(1 + 2s)f$ in the stator windings [17]. These are main signatures of a broken rotor bar in the stator currents, which are generally used as indexes for the fault diagnosis propose. To verify this, the normalized frequency spectra of stator line current are shown in Figure 7 for SCIM with one and six broken bars and healthy motor under 50% rate load. As seen, harmonic components at $(1\pm2s)f$ frequencies are clear in the spectra and their amplitudes are amplified due to the fault. Also, the amplitudes of the harmonics in SMCCM results are very close to those in experimental results.

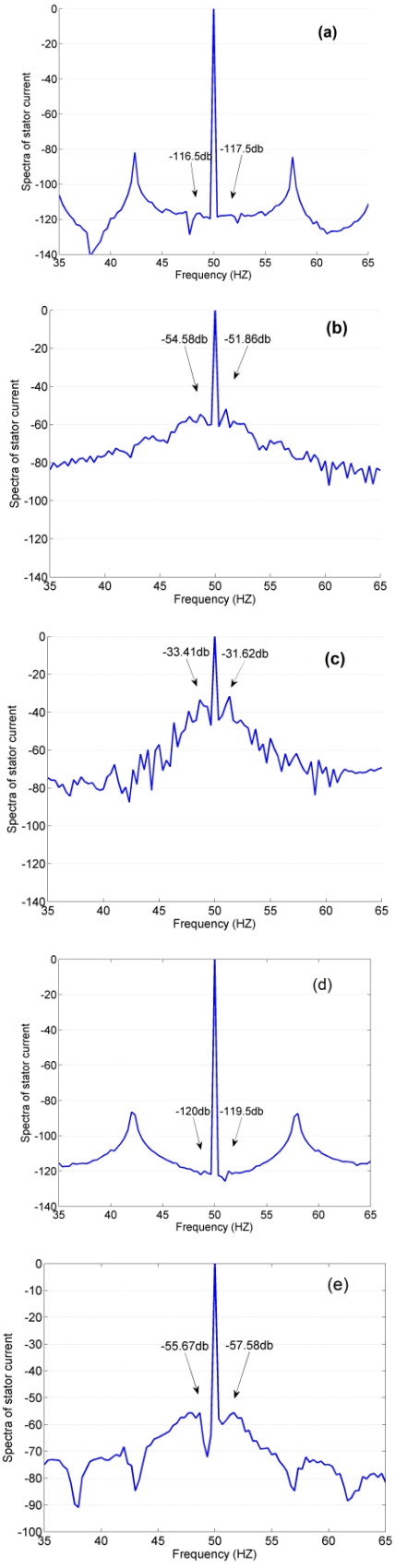

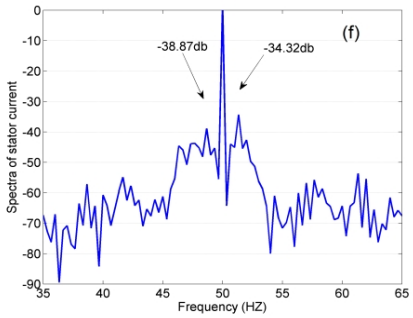

Figure 7. Normalized frequency spectra of stator line current obtained through simulation using SMCCM for SCIM on a) healthy motor, with b) one and c) six broken rotor bars and MCCM for SCIM on d) healthy motor, with e) one and f) six broken rotor bars under half rate load

4. SCIM PERFORMANCE DUE TO MAGNETIC SATURATION UNDER STATOR WINDING FAULT

Stator winding faults are usually related to insulation failure. Almost 30%-40% of the reported induction motor failures fall into this category [17]. Winding fault may take place in one of the following forms [20]:

- Turn to turn fault.
- Coil to coil fault.
- Phase to phase fault.
- Coil to ground fault.
- Open circuit fault.

In this case a stator winding turn to turn fault is considered. Generally, this fault is the initial cause of the other stator faults [20], therefore, it was appreciated by enormous research studies in the past [17, 21-25].

Short turns in one of the stator phases which can be modeled as a seventh phase with zero voltage in the machine equations. The turn functions are shown in Figure 8.Figure 9 shows variations of 7th phase self inductance versus K_{sat} and φ_f and also Figure 10 shows variations of mutual inductance between 7th phase and rotor mesh "1" and its derivative versus K_{sat} and θ_r via simulation using SMCCM for SCIM with 9 shorted turns under no load.

Figure 11 shows normalized frequency spectra of phase "a" stator line current obtained through simulation using SMCCM for healthy SCIM and for SCIM with 5 and 9 shorted turns under no load and also Figure 12 shows the same results as Figure 11 for phase "b". As seen, even harmonics of stator currents can be used for identification of stator winding turn-turn faults.

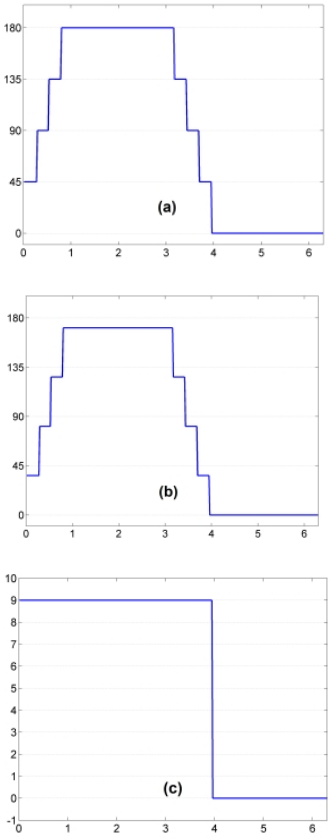

Figure 8. The turn functions of phase_a winding for a) healthy winding, b) faulty winding and c) 7th phase winding with 9 shorted turns, respectively

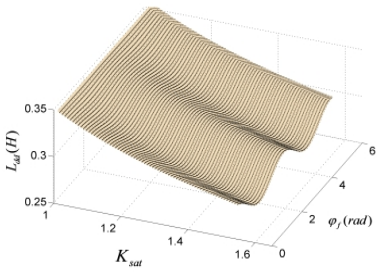

Figure 9. Phase "d" self inductance (L_{dd}) variation versus $K_{sat}$and j_f

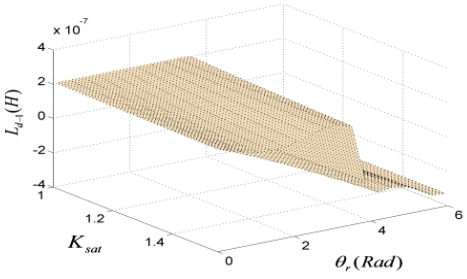

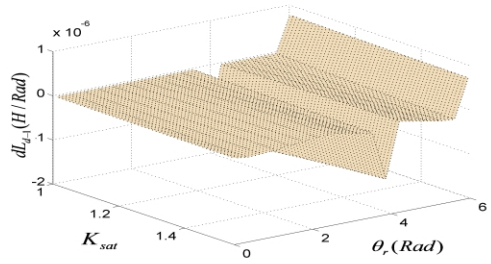

Figure 10. Mutual inductance between stator phase "d" and rotor mesh "1"(L_{d1} —top) and its derivative versus (dL_{d1}— bottom) variations versus K_{sat} and θ_r where $j_f = 0$.

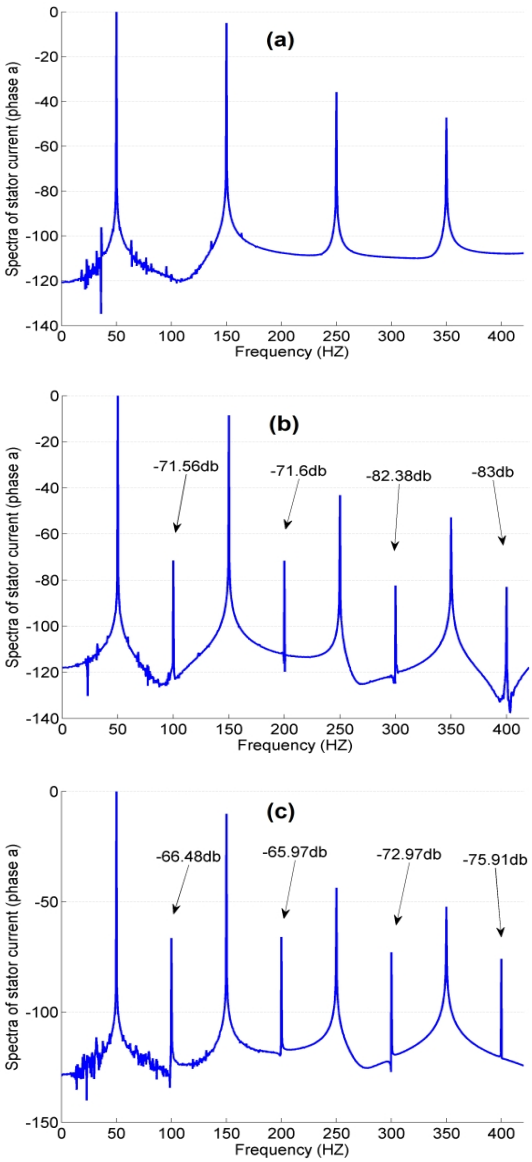

Figure 11. Normalized frequency spectra of phase "a" stator line current obtained through simulation using SMCCM for a) healthy SCIM and for SCIM with 5 and 9 shorted turns (b,c) respectively under no load

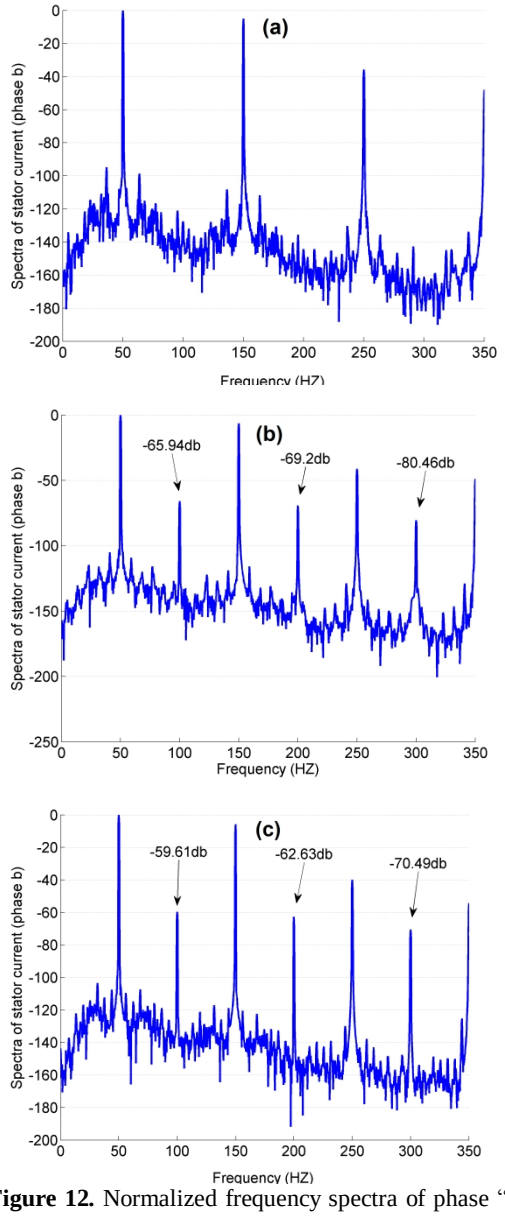

Figure 12. Normalized frequency spectra of phase "b" stator line current obtained through simulation using SMCCM for a) healthy SCIM and for SCIM with 5 and 9 shorted turns, (b,c) respectively under no load

5. CONCLUDING REMARKS

Rotor meshes flux-linkages, calculated in every simulation step by winding function approach, can be used to estimate the air gap flux density distribution. Then, space harmonic components of the air gap flux density can be determined using Fourier series analysis. The phase angle of the space fundamental harmonic is utilized to locate the air gap flux density during simulation of the faulty SCIMs. Also, the amplitude of this fundamental harmonic is applicable to evaluate the saturation factor more reasonably. Saturation may affect the performance and the fault indexes of the faulty SCIMs considerably and the new SMCCM is a helpful tool to analyze such effects.

6. REFERENCES

1. Bispo, D., Martins, L., de Resende, J.T. and de Andrade, D.A., "A new strategy for induction machine modeling taking into account the magnetic saturation", ***Industry Applications, IEEE Transactions on***, Vol. 37, No. 6, (2001), 1710-1719.
2. Tuovinen, T., Hinkkanen, M. and Luomi, J., "Modeling of saturation due to main and leakage flux interaction in induction machines", ***Industry Applications, IEEE Transactions on***, Vol. 46, No. 3, (2010), 937-945.
3. Tu, X., Dessaint, L.-A., Champagne, R. and Al-Haddad, K., "Transient modeling of squirrel-cage induction machine considering air-gap flux saturation harmonics", ***Industrial Electronics, IEEE Transactions on***, Vol. 55, No. 7, (2008), 2798-2809.
4. Nandi, S., "A detailed model of induction machines with saturation extendable for fault analysis", ***Industry Applications, IEEE Transactions on***, Vol. 40, No. 5, (2004), 1302-1309.
5. Ojaghi, M. and Faiz, J., "Extension to multiple coupled circuit modeling of induction machines to include variable degrees of saturation effects", ***Magnetics, IEEE Transactions on***, Vol. 44, No. 11, (2008), 4053-4056.
6. Levi, E., "Multiphase electric machines for variable-speed applications", ***Industrial Electronics, IEEE Transactions on***, Vol. 55, No. 5, (2008), 1893-1909.
7. Fnaiech, M.A., Betin, F., Capolino, G.-A. and Fnaiech, F., "Fuzzy logic and sliding-mode controls applied to six-phase induction machine with open phases", ***Industrial Electronics, IEEE Transactions on***, Vol. 57, No. 1, (2010), 354-364.
8. Joksimovic, G.M., Durovic, M.D., Penman, J. and Arthur, N., "Dynamic simulation of dynamic eccentricity in induction machines-finding function approach", ***Energy Conversion, IEEE Transactions on***, Vol. 15, No. 2, (2000), 143-148.
9. Faiz, J. and Tabatabaei, I., "Extension of winding function theory for nonuniform air gap in electric machinery", ***Magnetics, IEEE Transactions on***, Vol. 38, No. 6, (2002), 3654-3657.
10. Faiz, J. and Ojaghi, M., "Unified winding function approach for dynamic simulation of different kinds of eccentricity faults in cage induction machines", ***IET Electric Power Applications***, Vol. 3, No. 5, (2009), 461-470.
11. Nandi, S., "Detection of stator faults in induction machines using residual saturation harmonics", ***Industry Applications, IEEE Transactions on***, Vol. 42, No. 5, (2006), 1201-1208.
12. Faiz, J., Ebrahimi, B.M. and Toliyat, H.A., "Effect of magnetic saturation on static and mixed eccentricity fault diagnosis in induction motor", ***Magnetics, IEEE Transactions on***, Vol. 45, No. 8, (2009), 3137-3144.
13. Ojaghi, M., Sabouri, M., Faiz, J. and Ghorbanian, V., "Exact modeling and simulation of saturated induction motors with broken rotor bars fault using winding function approach", ***International Journal of Engineering-Transactions A: Basics***, Vol. 27, No. 1, (2013), 69.
14. Taheri, A., Rahmati, A. and Kaboli, S., "Efficiency improvement in dtc of six-phase induction machine by adaptive gradient descent of flux", ***Power Electronics, IEEE Transactions on***, Vol. 27, No. 3, (2012), 1552-1562.
15. Taheri, A., Rahmati, A. and Kaboli, S., "Comparison of efficiency for different switching tables in six-phase induction

motor dtc drive", ***Journal of Power Electronics***, Vol. 12, No. 1, (2012), 128-135.

16. Renukadevi, G. and Rajambal, K., "Performance investigation of multi-phase vsi with simple pwm switching techniques", ***International Journal of Engineering*, *Transactions C: Aspects*** Vol. 26, No. 1, (2013), 451-458.
17. Nandi, S., Toliyat, H.A. and Li, X., "Condition monitoring and fault diagnosis of electrical motors-a review", ***Energy Conversion, IEEE Transactions on***, Vol. 20, No. 4, (2005), 719-729.
18. Weili, L., Ying, X., Jiafeng, S. and Yingli, L., "Finite-element analysis of field distribution and characteristic performance of squirrel-cage induction motor with broken bars", ***Magnetics, IEEE Transactions on***, Vol. 43, No. 4, (2007), 1537-1540.
19. Sprooten, J. and Maun, J.-C., "Influence of saturation level on the effect of broken bars in induction motors using fundamental electromagnetic laws and finite element simulations", ***Energy Conversion, IEEE Transactions on***, Vol. 24, No. 3, (2009), 557-564.
20. Grubic, S., Aller, J.M., Lu, B. and Habetler, T.G., "A survey on testing and monitoring methods for stator insulation systems of low-voltage induction machines focusing on turn insulation problems", ***Industrial Electronics, IEEE Transactions on***, Vol. 55, No. 12, (2008), 4127-4136.
21. Wu, Q. and Nandi, S., "Fast single-turn sensitive stator inter-turn fault detection of induction machines based on positive and negative sequence third harmonic components of line currents", in Industry Applications Society Annual Meeting, IAS'08. IEEE, (2008), 1-8.
22. Gandhi, A., Corrigan, T. and Parsa, L., "Recent advances in modeling and online detection of stator interturn faults in electrical motors", ***Industrial Electronics, IEEE Transactions on***, Vol. 58, No. 5, (2011), 1564-1575.
23. Bouzid, M., Champenois, G., Bellaaj, N.M., Signac, L. and Jelassi, K., "An effective neural approach for the automatic location of stator interturn faults in induction motor", ***Industrial Electronics, IEEE Transactions on***, Vol. 55, No. 12, (2008), 4277-4289.
24. Faiz, J., Feyzi, M. and Abbasi, A., "Analysis of shaded pole induction motors considering asymmetrical flux distribution and saturation effects", ***International Journal of Engineering*, *Transactions A*** Vol. 9, No. 4 (1998), 189-196.
25. Moallem, M., Kiyoumarsi, A. and Hassanzadeh, M., "A novel technique on the analytical calculation of open-circuit flux density distribution in brushless permanent-magnet motor", ***International Journal of Engineering Transactions B***, Vol. 17, No. 1, (2004), 51-60.

APPENDIX

Short turns in one of the stator phases whichcan be modeled as a fourth phase with zero voltage in the machine equations. In both faulty and faultless motors with a sinusoidal distribution of windings, the self-inductance of each winding is proportional to the square of the count of turns, and the mutual inductance of five windings is proportional to the product of the counts of turns in two windings [21, 22]. The resultant mathematical model for a motor with short turns in phase "a"is derived and shown in Equations (2)-(16).

$$[V_S] = [R_S][I_S] + \frac{d}{dt}[y_S] \tag{2}$$

$$[0] = [R_r][I_r] + \frac{d}{dt}[y_r] \tag{3}$$

$$[y_S] = [L_{SS}][I_S] + [L_{Sr}][I_r] \tag{4}$$

$$[y_r] = [L_{rS}][I_S] + [L_{rr}][I_r] \tag{5}$$

$$[V_S] = \begin{bmatrix} V_a & V_b & V_c & V_x & V_y & V_z & 0 \end{bmatrix}^T \tag{6}$$

$$[I_S] = \begin{bmatrix} i_a & i_b & i_c & i_x & i_y & i_z & i_d \end{bmatrix}^T \tag{7}$$

$$[I_r] = \begin{bmatrix} i_1 & i_2 & \dots & i_R \end{bmatrix}^T \tag{8}$$

$$[y_s] = \begin{bmatrix} y_a & y_b & y_c & y_x & y_y & y_z & y_d \end{bmatrix} \tag{9}$$

$$[y_r] = \begin{bmatrix} y_1 & y_2 & \dots & y_R \end{bmatrix} \tag{10}$$

$$T_e = I_s^T \frac{\partial L'_{sr}}{\partial q} I_r \tag{11}$$

$$T_e - T_L = J\frac{dw}{dt} \tag{12}$$

$$[R_S] = \begin{bmatrix} (1-m)\times r_s & 0 & 0 & 0 & 0 & 0 & 0 \\ 0 & r_s & 0 & 0 & 0 & 0 & 0 \\ 0 & 0 & r_s & 0 & 0 & 0 & 0 \\ 0 & 0 & 0 & r_s & 0 & 0 & 0 \\ 0 & 0 & 0 & 0 & r_s & 0 & 0 \\ 0 & 0 & 0 & 0 & 0 & r_s & 0 \\ 0 & 0 & 0 & 0 & 0 & 0 & m\times r_s \end{bmatrix} \tag{13}$$

$$R_r = \begin{bmatrix} 2(R_b+R_e) & -R_b & 0 & \mathbf{K} & -R_b \\ -R_b & 2(R_b+R_e) & -R_b & \mathbf{K} & 0 \\ 0 & -R_b & 2(R_b+R_e) & \mathbf{K} & \mathbf{M} \\ \mathbf{M} & \mathbf{M} & \mathbf{M} & \mathbf{K} & \mathbf{M} \\ -R_b & 0 & \mathbf{K} & \mathbf{K} & 2(R_b+R_e) \end{bmatrix} \tag{14}$$

$$[L_{rr}] = \begin{bmatrix} L_{mr}+2(l_b+l_e) & L_{r12}-l_b & L_{r13} & \mathbf{L} & L_{r1n}-l_b \\ L_{r21}-l_b & L_{mr}+2(l_b+l_e) & L_{r23}-l_b & \mathbf{L} & L_{r2n} \\ L_{r31} & \mathbf{L} & \mathbf{L} & \mathbf{L} & \mathbf{M} \\ \mathbf{M} & \mathbf{M} & \mathbf{M} & \mathbf{M} & \mathbf{M} \\ L_{rn1} & L_{rn2} & L_{rn3} & \mathbf{L} & L_{mr}+2(l_b-l_e) \end{bmatrix} \tag{15}$$

$$[L_{SS}]=\begin{bmatrix} (1-m^2)\times L_{aa}+(1-m)\times L_{ls} & (1-m)\times L_{ab} & (1-m)\times L_{ac} & (1-m)\times L_{ax} & (1-m)\times L_{ay} & (1-m)\times L_{az} & m\times(1-m)\times L_{ad} \\ (1-m)\times L_{ba} & L_{bb}+L_{ls} & L_{bc} & L_{bx} & L_{by} & L_{bz} & m\times L_{bd} \\ (1-m)\times L_{ca} & L_{cb} & L_{cc}+L_{ls} & L_{cx} & L_{cy} & L_{cz} & m\times L_{cd} \\ (1-m)\times L_{xa} & L_{xb} & L_{xc} & L_{xx}+L_{ls} & L_{xy} & L_{xz} & m\times L_{xd} \\ (1-m)\times L_{ya} & L_{yb} & L_{yc} & L_{yx} & L_{yy}+L_{ls} & L_{yz} & m\times L_{yd} \\ (1-m)\times L_{za} & L_{zb} & L_{zc} & L_{zx} & L_{zy} & L_{zz}+L_{ls} & m\times L_{zd} \\ m\times(1-m)\times L_{da} & m\times L_{db} & m\times L_{dc} & m\times L_{dx} & m\times L_{dy} & m\times L_{dz} & m^2\times L_{dd}+m\times L_{ls} \end{bmatrix} \quad (16)$$

Magnetic Saturation Impacts on Fault Analysis of Squirrel-cage Six Phases Induction Motors Using Winding Function Approach

A. Taheri, M. Sabouri

Department of Electrical Engineering, University of Zanjan, Zanjan, Iran

P A P E R I N F O

Paper history:
Received 10 November 2013
Received in revised form 15 March 2014
Accepted 22 May 2014

Keywords:
6-Phases Squirrel-cage Induction Motors
Saturation Effect
Rotor Fault
Stator Fault
Winding Function Approach

چکیده

مدل مدارهای مزدوج چندگانه (MCCM) موتورهای القایی قفس سنجابی (SCIM) یا روش تابع سیم پیچ، مفصل ترین و کاملترین مدل استفاده شده برای آنالیز عملکرد موتورهای القایی قفس سنجابی می باشد. قبلا از این روش در مقالات مختلف برای موتورهای القایی قفس سنجابی 3 فاز استفاده شده است اما این مقاله مدل فوق را به موتورهای القایی 6 فاز بسط داده است. شبیه سازی های مختلفی از عیوب گوناگون بر روی موتورهای القایی 6 فاز انجام گرفته شده است و سپس نتایج بدست آمده از شبیه سازی ها، ارائه گردیده است. نوآوری این مقاله شبیه سازی برای اولین بار موتورهای القایی قفس سنجابی 6 فاز با روش تابع سیم پیچ با در نظر گرفتن اثر اشباع مغناطیسی با عیوب سیم پیچی استاتور و روتور با میله شکسته شده می باشد که نتایج بصورت دقیق به خوبی نشان داده شده اند.

doi: 10.5829/idosi.ije.2014.27.09c.05